

Cesium-137 deposition and contamination of Japanese soils due to the Fukushima nuclear accident

Tepei J. Yasunari^{a,1}, Andreas Stohl^b, Ryugo S. Hayano^c, John F. Burkhardt^{b,d}, Sabine Eckhardt^b, and Tetsuzo Yasunari^e

^aUniversities Space Research Association, Goddard Earth Sciences Technology and Research, Columbia, MD 21044; ^bNorwegian Institute for Air Research, P.O. Box 100, N-2027 Kjeller, Norway; ^cDepartment of Physics, University of Tokyo, 7-3-1 Hongo, Bukyo-ku, Tokyo 113-0033, Japan; ^dSierra Nevada Research Institute, University of California, Merced, 5200 North Lake Road, Merced, CA 95343; and ^eHydrospheric Atmospheric Research Center, Nagoya University, Nagoya, Aichi 464-8601, Japan

Edited by James E. Hansen, Goddard Institute for Space Studies, New York, NY, and approved October 5, 2011 (received for review July 25, 2011)

The largest concern on the cesium-137 (¹³⁷Cs) deposition and its soil contamination due to the emission from the Fukushima Daiichi Nuclear Power Plant (NPP) showed up after a massive quake on March 11, 2011. Cesium-137 (¹³⁷Cs) with a half-life of 30.1 y causes the largest concerns because of its deleterious effect on agriculture and stock farming, and, thus, human life for decades. Removal of ¹³⁷Cs contaminated soils or land use limitations in areas where removal is not possible is, therefore, an urgent issue. A challenge lies in the fact that estimates of ¹³⁷Cs emissions from the Fukushima NPP are extremely uncertain, therefore, the distribution of ¹³⁷Cs in the environment is poorly constrained. Here, we estimate total ¹³⁷Cs deposition by integrating daily observations of ¹³⁷Cs deposition in each prefecture in Japan with relative deposition distribution patterns from a Lagrangian particle dispersion model, FLEXPART. We show that ¹³⁷Cs strongly contaminated the soils in large areas of eastern and northeastern Japan, whereas western Japan was sheltered by mountain ranges. The soils around Fukushima NPP and neighboring prefectures have been extensively contaminated with depositions of more than 100,000 and 10,000 MBq km⁻², respectively. Total ¹³⁷Cs depositions over two domains: (i) the Japan Islands and the surrounding ocean (130–150°E and 30–46°N) and, (ii) the Japan Islands, were estimated to be more than 5.6 and 1.0 PBq, respectively. We hope our ¹³⁷Cs deposition maps will help to coordinate decontamination efforts and plan regulatory measures in Japan.

aerosol | dispersion modeling | radioactive fallout

A catastrophic earthquake and tsunami occurred on March 11, 2011, which caused destruction in northeastern Japan and severely damaged the Fukushima Daiichi Nuclear Power Plant (NPP). This event led to emissions of radioactive materials from the NPP (1), albeit at unknown and likely strongly varying release rates (1–3). Among these materials, with a half-life of 30.1 y (4), cesium-137 (¹³⁷Cs) causes the largest concerns because of its deleterious effect on agriculture and stock farming, and, thus, human life for decades. Removal of ¹³⁷Cs-contaminated soils or land use limitations in areas where removal is not possible is, therefore, an urgent issue. The Japanese government, general public, and scientists have been waiting for the information of the spatial distributions of ¹³⁷Cs deposition and its soil contamination over all of Japan.

The aerosol-bound ¹³⁷Cs can be removed from the atmosphere and brought to the surface by dry or wet deposition. Analysis of data collected after the Chernobyl accident has shown that ¹³⁷Cs adsorbed in the top soil layer can remain there for many years (5, 6), restricting land use, e.g., for food production, of highly contaminated areas for a long time. To minimize the impacts on human health of soil contamination in Japan due to the Fukushima NPP accident, spatial maps of ¹³⁷Cs deposition and concentrations in soil are urgently needed. Sporadic sampling of the soils in and around Fukushima prefecture has been carried out after the NPP accident under the instruction by the Ministry of Education, Culture, Sports, Science and Technology (MEXT)

(7) and others (Table S1). However, it is impossible to fully capture the distribution of ¹³⁷Cs deposition across Japan from a limited number of in situ measurements alone. On the other hand, reliable estimates using dispersion models are also not available because of the largely unknown source term. Not only is the total release of ¹³⁷Cs from the damaged NPP poorly known, but also its variation with time is even more uncertain. Although first attempts to estimate it have been made (2) and another study tried to estimate its deposition based on the previous study (2) over the limited areas around Fukushima prefecture with a regional chemical transport model (8), these estimates on the emission rate are highly uncertain and the discussion on deposition over all of Japan has not been made.

In this study we quantitatively estimate the spatial distribution of the ¹³⁷Cs deposition and its soil contamination over all of Japan. We take relative deposition distribution patterns from a Lagrangian particle dispersion model, FLEXPART (*Materials and Methods* and *SI Text*) (9), using a constant source term [as assumed also in some simulations because of high uncertainty of the emission amount (10–16)]. We fuse daily varying observations of ¹³⁷Cs deposition in each Japanese prefecture (17) into the modeled deposition fields to obtain quantitative deposition estimates.

Results

Our estimate of ¹³⁷Cs deposition is made for the period between March 20 and April 19 because no observations of ¹³⁷Cs deposition were made between March 12 and 17 and the dispersion model did not simulate any depositions at the observation locations on March 18 and 19 (Fig. S1). Thus, our quantitative estimates do not include the first 8 d after the NPP accident, yet for that period we provide relative contributions to the deposition. In Fig. 1A we show the relative contribution map of the deposition over the period when our estimate was not applicable. It shows that before March 20, potentially contaminated air masses were mainly transported toward the Pacific Ocean and ¹³⁷Cs deposition would have occurred mostly over the ocean, except for Fukushima prefecture and some neighboring provinces. Between March 20 and April 19 (Fig. 1B), a much wider area was effected by the deposition. In particular, eastern and northeastern parts of Japan had a greater potential for ¹³⁷Cs deposition, whereas in western Japan the potential for ¹³⁷Cs deposition was low. Overall, however, the highest potential deposition occurred over the Pacific Ocean, where a few observations of ¹³⁷Cs deposition exist (18), showing that winds were generally quite favorable and carried most radiation away from populated areas.

Author contributions: T.J.Y. designed research; T.J.Y., A.S., J.F.B., and S.E. performed research; T.J.Y. and R.S.H. analyzed data; and T.J.Y., A.S., J.F.B., and T.Y. wrote the paper.

The authors declare no conflict of interest.

This article is a PNAS Direct Submission.

Freely available online through the PNAS open access option.

¹To whom correspondence should be addressed: E-mail: tyasunari@usra.edu.

This article contains supporting information online at www.pnas.org/lookup/suppl/doi:10.1073/pnas.1112058108/-DCSupplemental.

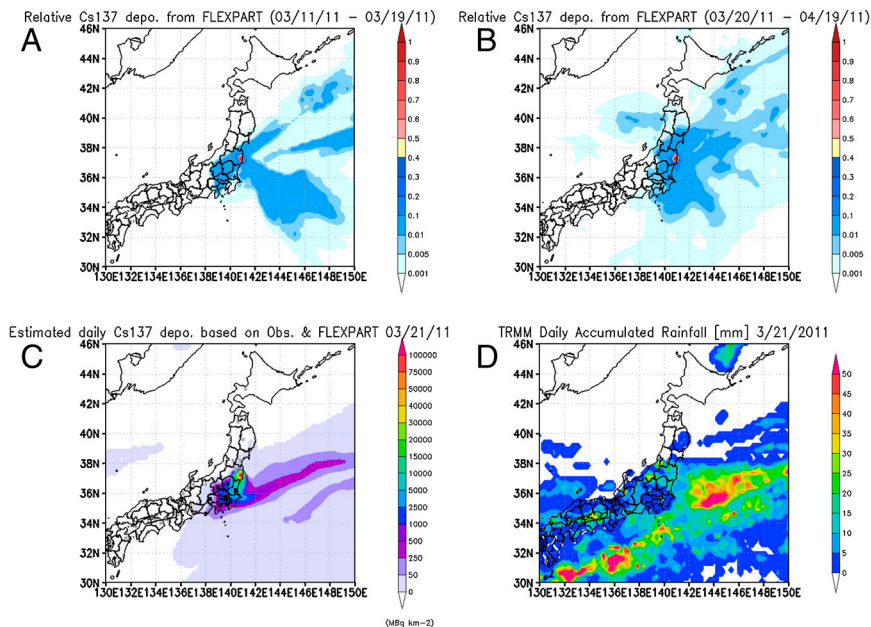


Fig. 1. Cesium-137 deposition maps. (A) Relative deposition contributions between March 11 and 19, showing the areas potentially effected by ^{137}Cs before the start of measurements. The sums of the depositions during the period were divided by the maximum deposition in the accumulated field. (B) The same as in A, but for March 20–April 19. (C) An example of estimated daily deposition of ^{137}Cs on March 21. Squares in black denote the observation locations in each prefecture (Table S2). (D) Daily accumulated rainfall on March 21 by TRMM.

From March 20, we can estimate ^{137}Cs deposition fields over Japan more reliably because daily observations have been made in most Japanese prefectures (17) (Table S2). For days from March 20, we create deposition estimates using scaled model values [hereafter called, deposition ratio (DR); see *Materials and Methods*] from a constant source term simulation in conjunction with the measurements from the MEXT observation network (17). An example of a three-hourly DR animation map is available in *Movie S1*. For periods when the simulated daily DR value is close to zero yet deposition is observed, a threshold factor is employed in Eq. 2 (*Materials and Methods* and *SI Text*). In such cases, a minimum positive deposition ratio value, hereafter called DR threshold (DRT), needs to be used to derive the scaling (*Materials and Methods* and *SI Text*). The choice of this DRT is subjective and also affects the estimated deposition amount in our method. After performing comparisons with the observed depositions in each prefecture (*SI Text*, Fig. S2, and Table S3), we used a DRT of 0.005 for the best guess estimate of daily deposition between March 20 and April 19 (*Movie S2*) but we also report derived deposition estimates for other DRT values.

The simulated distribution of ^{137}Cs deposition is closely linked to precipitation as shown for the case of March 21 (Fig. 1 C and D). The highest deposition values downwind of the NPP are clearly aligned with satellite-observed precipitation by tropical rainfall measuring mission (TRMM, 3B42 V6 product) in a frontal rain band, which causes washout of the radionuclides (*Movie S2* and *S3*). Comparison of daily observed precipitation fields with the estimated deposition maps shows that ^{137}Cs deposition is simulated mainly when frontal rain bands pass over Japan (*Movie S2*). It was reported previously (19) that around 90% of the total deposition of ^{137}Cs occurs with precipitation. Thus, the general agreement between observed precipitation and simulated deposition confirms that the model captures the main deposition events, which is also consistent with the discussion from the study by using a regional chemical transport model (8). The daily ^{137}Cs deposition was frequently detected at observatories (17) in the eastern and northeastern prefectures of Japan from March 20. Furthermore, large increases of atmospheric radioactivity in the prefectures around Fukushima were observed (20) on March 22 (Fig. S3), probably reflecting ground shine

radiation from the radionuclides deposited during the rainfall event on March 21 (Fig. 1 C and D).

Maps of the total ^{137}Cs deposition between March 20 and April 19 are shown in Fig. 24. As a general characteristic, most of the eastern parts of Japan were effected by a total ^{137}Cs deposition of more than $1,000 \text{ MBq km}^{-2}$. Our estimates show that the area around NPP in Fukushima, secondarily effected areas (Miyagi and Ibaraki prefectures), and other effected areas (Iwate, Yamagata, Tochigi, and Chiba prefectures) had ^{137}Cs depositions of more than $100,000$, $25,000$, and $10,000 \text{ MBq km}^{-2}$, respectively. Airborne and ground-based survey measurements jointly carried out by MEXT and the US Department of Energy (DOE) (21) show high ^{137}Cs deposition amounts were observed northward and up to a distance of 80 km from Fukushima NPP. It was estimated from the first measurement that by April 29, more than $600,000 \text{ MBq km}^{-2}$ had been deposited in the area, which is greater than our estimate of less than $500,000 \text{ MBq km}^{-2}$ (Fig. 24), yet well within the range of uncertainty of our method (Fig. S4). Furthermore, because no observations on daily deposition were available before March 27 in Fukushima City (Fig. 2B) and no daily deposition observations around NPP, our estimates are expected to underestimate the total deposition in the vicinity of the NPP. In conducting sensitivity studies with DRT, our estimates provide values on the similar order of the MEXT/DOE observations using a DRT value of 0.001 (Fig. S4).

Using an approximate relationship between ^{137}Cs deposition and its topsoil concentration (22) [conversion coefficient (CC) of $53 \pm 15 \text{ kg m}^{-2}$] (Fig. S5), we converted the estimated depositions into topsoil concentrations (Fig. 3, *Movie S4*, and Table S4).

We compared ^{137}Cs concentrations in the topsoil derived from both observed ^{137}Cs deposition values (17) and from our estimates, with direct measurements of ^{137}Cs concentrations in soils and grasses with a soil-to-grass transfer factor of 0.13 (23) (*SI Text* and Table S1) (Fig. 4). The MEXT deposition-based soil contamination tends to be lower than the soil- and grass-based samplings because of the latter including the time period just after the NPP accident. Our scaled model deposition fields agree well with both the point measurements including the MEXT areal surveys and other available observations (Fig. 4), generally falling in the range between the two techniques. If the soil contaminations closer to

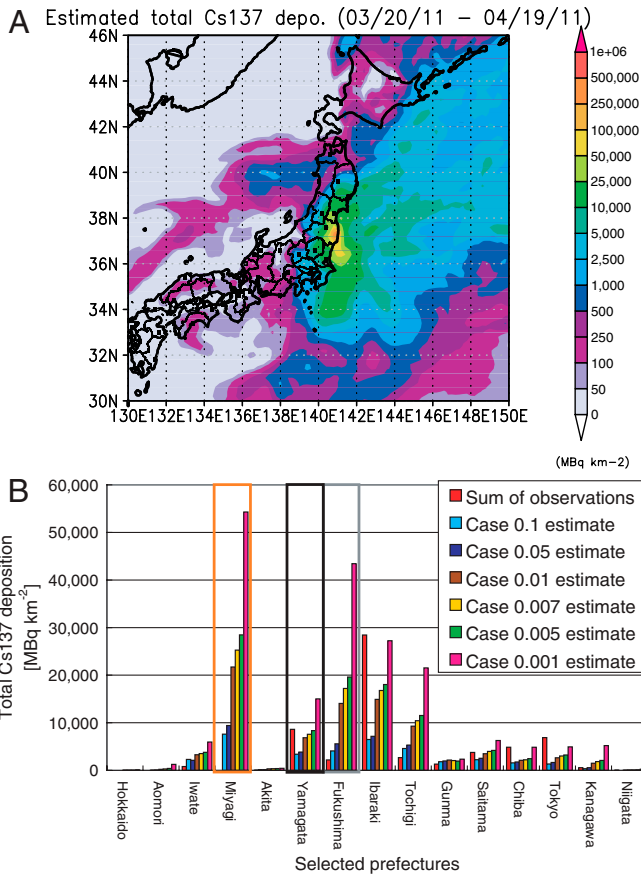


Fig. 2. Total deposition of ^{137}Cs . (A) Gridded total ^{137}Cs deposition values for the period March 20–April 19 using our reference DRT value of 0.005. Outputs with $0.2^\circ \times 0.2^\circ$ were interpolated to finer grid using cubic interpolation. Squares in black denote the observation locations in each prefecture (Table S2). (B) Comparisons between total observed depositions for the period March 20–April 19 and estimates at the grid point of each observatory location (Table S2) in the selected prefectures, using different DRT values to derive the scaling factor for the model output. Orange, gray, and black boxes denote no observation (Miyagi) and missing observations (Yamagata, between March 29 and April 3; Fukushima, before March 27 and April 4), respectively.

the Fukushima NPP are included, the observed soil contamination has a wider range of 190–310,000 Bq kg^{-1} with mean and median values of 20,575 and 5,750 Bq kg^{-1} , respectively. The observations in Fukushima City give a lower range of 620–21,000 Bq kg^{-1} (mean, 5,969 Bq kg^{-1} ; median, 4,200 Bq kg^{-1}). Our estimated distributions were within the range of the observations around the NPP, but close to the lower bound (Fig. 3 and Fig. 4). From the sporadic observations (7, 21) (Table S1) and our estimate in this study, Fukushima prefecture as a whole is highly contaminated, especially to the northwest of the NPP, with soil ^{137}Cs concentrations above 1,000 Bq kg^{-1} throughout the east prefecture from our estimate (Fig. 3). Neighboring prefectures are less contaminated, but ^{137}Cs concentrations there are still above 250 Bq kg^{-1} in most of the areas. Thus our approach provides a necessary estimate of deposition beyond the immediate area of the Fukushima prefecture, where monitoring activities are less intensive.

Discussion

There are many important agricultural regions in Japan. In Japan, the limit for the sum of ^{134}Cs and ^{137}Cs concentrations (as total cesium) in soil is 5,000 Bq kg^{-1} under the Food Sanitation Law (24). Considering that about half (2,500 Bq kg^{-1}) of the total radioactive cesium deposition is due to ^{137}Cs , the east Fukushima prefecture exceeded this limit and some neighboring prefectures such as Miyagi, Tochigi, and Ibaraki are partially close

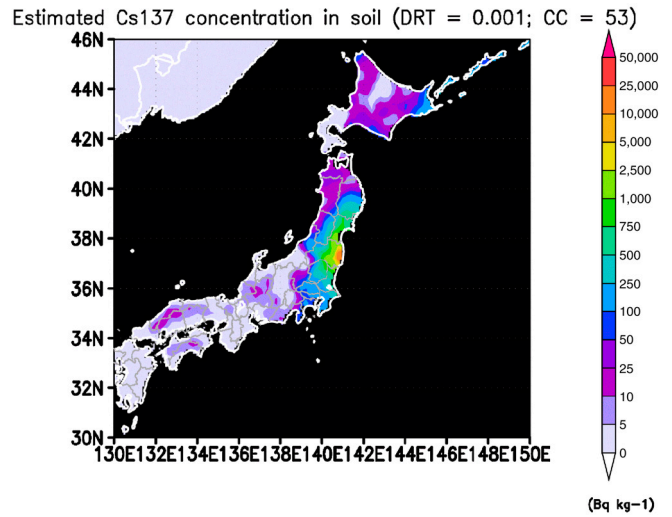


Fig. 3. The ^{137}Cs concentration in soil. We used DRT of 0.001 and CC of 53 kg m^{-2} . Outputs with $0.2^\circ \times 0.2^\circ$ were interpolated to finer resolution using cubic interpolation. The Merged IBCAO/ETOPO5 Global Topographic Data Product (25) was used to mask out ocean area below 0 m above sea level (a.s.l.).

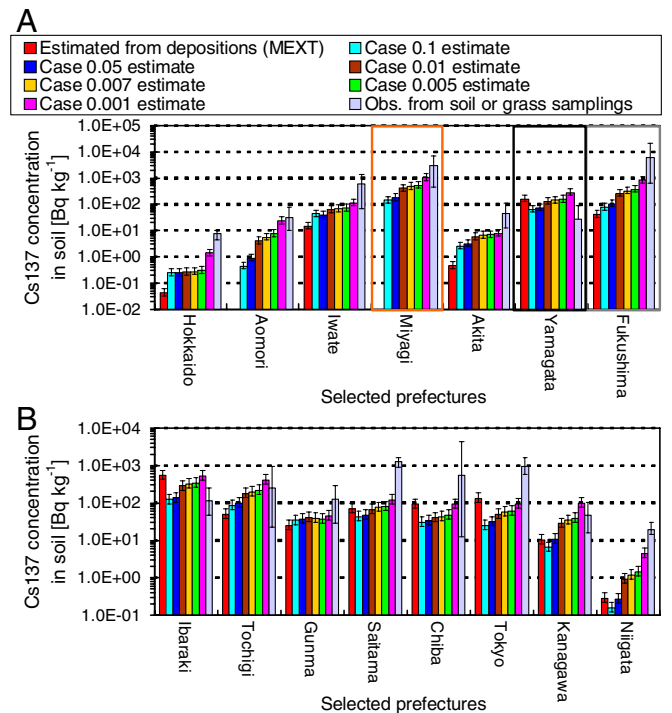


Fig. 4. Atmospheric, soil, and grass observation-based Cs-137 concentrations, and estimates based on the scaled model output and for different DRT values used for the scaling. (A) Comparisons in northern prefectures. Aomori and Miyagi prefectures had no ^{137}Cs detections on the daily deposition data and no measurements, respectively. The minimum value in Yamagata prefecture is no detection and no lower error bar is shown. (B) The same as in A, but around Kanto area. Lower and upper error bars denote minimum and maximum concentrations using CC of 68 and 38 kg m^{-2} based on Fig. S5, respectively. Orange, gray, and black boxes denote no observation (Miyagi) and missing observations (Yamagata, between March 29 and April 3; Fukushima, before March 27 and April 4), respectively. A soil-to-grass transfer factor of 0.13 (23) was used to convert grass to soil contamination. For Fukushima prefecture, only the soil observations in Fukushima City were used, excluding other observations close to the Fukushima NPP. The data source for the comparisons are summarized in Table S1.

to the limit under our upper bound estimate (Movie S4) and, therefore, local-scale exceedance is likely given the strong spatial variability of ^{137}Cs deposition. For those three prefectures, detailed soil sampling is recommended in the near future. Estimated and observed contaminations in the western parts of Japan were not as serious, even though some prefectures were likely effected to some extent (Fig. 3, Movie S4, and Table S4). Concentrations in these areas are below 25 Bq kg^{-1} , which is far below the threshold for farming. However, we strongly recommend each prefecture to quickly carry out some supplementary soil samplings at city levels to validate our estimates even if the concentrations are low.

The relatively low contamination levels over western Japan can be well explained by the Japanese topography. The eastern and northeastern parts of Japan are surrounded by mountain ranges such as the Kanto, Echigo, and Ohwu mountain ranges (Fig. S6) (25), which, to a large extent, sheltered the northwestern and western parts of Japan from the dispersion of radioactive material. It is worth noting, however, that relatively higher contamination levels can be seen over the Hida, Chugoku, and Shikoku mountain ranges (Fig. 3, Fig. S6, and Movie S4), probably due to orographic enhancement of precipitation and, thus, wet deposition of ^{137}Cs . In Hokkaido, to the north of Japan's main island, both lower altitude and higher altitudes such as the Yubari and Hidaka mountain ranges are effected by ^{137}Cs deposition, partially due to direct transport from the Fukushima NPP via the Pacific Ocean as shown in Movies S1 and S2 and also as simulated by another atmospheric transport model (12).

We estimate that a total of more than 5.6 and 1.0 PBq ^{137}Cs were deposited over Japan and the surrounding ocean ($130\text{--}150^\circ\text{E}$ and $30\text{--}46^\circ\text{N}$), and the Japan Islands in this domain only, respectively (Fig. 24). Although the estimate for the larger domain is quite uncertain because it is constrained only by measurements in Japan, these numbers are consistent with a suspected total release of about 12 PBq ^{137}Cs (2). Most of the deposition occurred over the Pacific Ocean, yet soil concentrations of ^{137}Cs are above 100 Bq kg^{-1} over large areas of eastern Japan (Fig. 3). According to our results, food production in eastern Fukushima prefecture is likely severely impaired by the ^{137}Cs loads of more than $2,500 \text{ Bq kg}^{-1}$ (upper limit of farming) and also partially impacted in neighboring provinces such as Iwate, Miyagi, Yamagata, Niigata, Tochigi, Ibaraki, and Chiba, where values of more than 250 Bq kg^{-1} cannot be excluded (Fig. 3 and Movie S4). Notice also that our estimates are based on a transport model driven with meteorological analysis data from a global model. Such a model cannot fully capture all complexities of the regional wind field over Japan and, in particular, does not resolve the high spatiotemporal variability of precipitation. Therefore, we expect the true soil contamination across Japan to be considerably more variable than in our estimate. Even in regions where we find relatively low soil contamination levels, hot spots with high concentrations (e.g., due to convective rain fall, orographic enhancement of rainfall, or fine-grain soil flow by rainwater on the ground) may be possible. In contrast, relatively clean patches may also be present in areas with high overall contamination levels. Despite these shortcomings, we expect our results to be useful for regulatory measures and for guiding monitoring activities toward areas with expected high ^{137}Cs burdens. We hope this study will contribute to understanding the contamination issue in Japan.

Materials and Methods

Observations of Cesium-137 Deposition and Concentration in Soil in each Prefecture. From March 18, MEXT has been observing daily radioactivity levels in deposition in most of the prefecture (17). The exact coordinates of the sampling locations were individually accessible through our contacts to MEXT (Table S2). The deposition data between March 18 and 19 were not used in our estimate because of no depositions at observatories from the modeled DR maps as mentioned in the main text. In some prefectures, data were missing or unavailable [Miyagi, March 18–April 19 (completely no observations);

Yamagata, March 29–April 3; Fukushima, March 18–March 26 and April 4; Gifu, March 24, 25, 27, 28, and 30; Nara, March 18–21 and April 15–18; Oita, March 22–26].

FLEXPART and Estimated ^{137}Cs Deposition. FLEXPART (9) is a Lagrangian particle dispersion model simulating transport, diffusion, dry and wet deposition, and radioactive decay of radioactive materials such as ^{131}I , ^{137}Cs , and ^{133}Xe (See <http://transport.nilu.no> for further details on FLEXPART). In this study, continuous emission from the Fukushima Daiichi NPP was assumed after 1800 hours coordinated universal time (UTC) on March 11, 2011. The simulation ended at 0000 hours UTC on April 20. FLEXPART was forced with the European Center for Medium-Range Weather Forecasts (ECMWF) operational analysis data with a global resolution of $1^\circ \times 1^\circ$ and $0.18^\circ \times 0.18^\circ$ for $120\text{--}168^\circ\text{E}$ and $25\text{--}50^\circ\text{N}$. The output had a resolution of $0.2^\circ \times 0.2^\circ$ and was recorded every 3 h (SI Text).

For each day, we first normalized the modeled daily accumulated deposition in each grid cell with the maximum accumulated deposition value for the model domain, hereafter called daily deposition ratio (DDR) maps:

$$DDR_{(x,y)} = \frac{1}{FPD_{\max,i}} \sum_{i=1}^T FPD_{(x,y),i}, \quad [1]$$

where $FPD_{(x,y),i}$ is the three-hourly modeled deposition in grid cell (x,y) and FPD_{\max} is the maximum daily deposition value found in the entire model domain. T is the number of model output timesteps per day ($T = 8$). Daily gridded deposition values of ^{137}Cs were estimated by scaling the DDR map with available daily observed ^{137}Cs depositions in each prefecture by MEXT (17) by the following equation:

$$Depo_{(x,y)} = \frac{DDR_{(x,y)}}{N} \sum_{i=1}^N \frac{Depo_{i(Obs.)}}{DDR_{i(Obs.Loc.)}}, \quad [2]$$

where $Depo_{(x,y)}$ is the estimated daily total ^{137}Cs deposition in grid cell (x,y) , $Depo_{i(Obs.)}$ is the observed ^{137}Cs deposition at location i (Table S2), $N \leq 47$ is the number of available counts on a certain day in Japan's 47 prefectures, $DDR_{i(Obs.Loc.)}$ is the $DDR_{(x,y)}$ in the grid point where ^{137}Cs deposition was observed, and $DDR_{(x,y)}$ is the DDR in grid cell (x,y) . Only the cases with both the observed deposition and the $DDR_{i(Obs.Loc.)}$ not equal to zero at each observatory location were used for counting N on each day. Because the $Depo_{i(Obs.)}$ to $DDR_{i(Obs.Loc.)}$ scaling factor in Eq. 2 becomes infinite when the simulated DDR value is close to zero but deposition is actually observed, a minimum positive DDR value, DRT, needs to be used to derive the scaling. Several DRTs of 0.001, 0.005, 0.007, 0.01, 0.05, and 0.1 for $DDR_{i(Obs.Loc.)}$ within the simulation domain on each day were used to avoid abnormally high $Depo_{(x,y)}$ values due to dividing by small values (SI Text). If $DDR_{i(Obs.Loc.)}$ at a certain grid point was less than a DRT value, $DDR_{i(Obs.Loc.)}$ was set to the DRT value.

For computing total ^{137}Cs deposition between March 20 and April 19, we corrected all values to April 19 using a half-life of ^{137}Cs of 30.1 y (4). The sum of all the daily observed or estimated ^{137}Cs depositions is the total ^{137}Cs deposition (Fig. 2 and Fig. S4A).

Observations on ^{137}Cs Concentrations in Soil and Grass. For comparison with our estimates, measurements of ^{137}Cs concentrations in soil or grass were used (SI Text and Table S1). Mean transfer factor of soil-to-grass of 0.13, which was obtained from the observations in Japanese soil and grass, was used to convert grass contamination to soil equivalent contamination (grass contamination divided by the transfer factor) (23). The times and locations of those samplings varied. To cover the time period of our study (March 20–April 19), we also used some soil samples from later dates, but we did not use any data after May 19. Notice also that the soil samples were also effected by ^{137}Cs deposition before March 20 (SI Text). Some observatories measured total cesium concentration including both ^{137}Cs and ^{134}Cs . In that case, we assumed that half of the total Cs was ^{137}Cs .

To convert the ^{137}Cs deposition into soil concentration, soil depth and density information are needed. However, it is currently difficult to obtain this information across all of Japan. There is an empirical relationship on the ratio between ^{137}Cs concentration and deposition from 0 to 5 cm soil, paddy soil, and field soil samples (22) (Fig. S5). We considered the mean value of the ratio as CC of $53 \pm 15 \text{ kg m}^{-2}$ reflecting the 5-cm depth soil information and its density. Our estimated CC value is close to the CC value of 65 kg m^{-2} assumed by MEXT (26) with 5-cm soil and a soil density of $1,300 \text{ kg m}^{-3}$.

Dividing our estimated deposition ($\text{MBq km}^{-2} = \text{Bq m}^{-2}$) by the CCs, we empirically obtained the mean ^{137}Cs concentration in soil (Bq kg^{-1}).

ACKNOWLEDGMENTS. Useful comments were obtained from K.-M. Kim Morgan State University (MSU)/Goddard Earth Sciences Technology and Research (GESTAR) and Q. Tan Universities Space Research Association (USRA)/GESTAR. Daily deposition of radioactive materials, atmospheric radiations, and concentrations in soil used in this study were observed by the Ministry of Education, Culture, Sports, Science, and Technology (MEXT),

each prefecture in Japan, the Ministry of Agriculture, Forestry and Fisheries (MAFF), and Prof. Yamazaki et al. at Kinki University. We also appreciate all the people working on these measurements. The tropical rainfall measuring mission (TRMM, 3B42 V6 product) data used in this study were acquired using the Goddard Earth Sciences (GES)-Data and Information Services Center (DISC) as part of the National Aeronautics and Space Administration's GES-DISC. The Grid Analysis and Display System (GrADS) was used for plotting. This paper was partially supported by Universities Space Research Association.

1. Nuclear and Industrial Safety Agency (2011). Available at: <http://www.nisa.meti.go.jp/english/files/en20110321-1.pdf>. March 20, 2011.
2. Chino M, et al. (2011) Preliminary estimation of release amount of ^{131}I and ^{137}Cs accidentally discharged from the Fukushima Daiichi Nuclear Power Plant into the atmosphere. *J Nucl Sci Technol (Tokyo)* 48:1129–1134.
3. Hoetzlein RC (2011) Fukushima radiation—comparison map., Available at: <http://www.rchoetzlein.com/theory/2011/fukushima-radiation-comparison-map/>.
4. Unterweger MP, Hoppes DD, Schima FJ (1992) New and revised half-life measurements results. *Nucl Instrum Methods Phys Res Sect A* 312:349–352.
5. Filipovic-Vincekovic N, Barisic D, Masic N, Lulic S (1991) Distribution of fallout radionuclides through soil surface layer. *J Radioanal Nucl Chem* 148:53–62.
6. Giani L, Helmers H (1997) Migration of Cesium-137 in typical soils of North Germany ten years after the Chernobyl accident. *Z Pflanz Bodenkunde* 160:81–83.
7. Japanese Ministry of Education, Culture, Sports, Science, and Technology (MEXT) (2011) Readings of environmental radiation level of dust and soil by monitoring in schools in Fukushima Prefecture., Available at: <http://www.mext.go.jp/english/incident/1305657.htm>.
8. Morino Y, Ohara T, Nishizawa M (2011) Atmospheric behavior, deposition, and budget of radioactive materials from the Fukushima Daiichi nuclear power plant in March 2011. *Geophys Res Lett* L00G11.
9. Stohl A, Forster C, Frank A, Seibert P, Wotawa G (2005) The Lagrangian particle dispersion model FLEXPART version 6.2. *Atmos Chem Phys* 5:2461–2474.
10. Japanese Ministry of Education, Culture, Sports, Science, and Technology (MEXT) (2011) System for prediction of environment emergency dose information (SPEEDI)., Available at: http://www.nsc.go.jp/mext_speedi/index.html (in Japanese).
11. Japan Meteorological Agency (2011) Environmental Emergency Response., Available at: http://www.jma.go.jp/jma/kokusai/eeer_list.html.
12. Takemura T, et al. (2011) A numerical simulation of global transport of atmospheric particles emitted from the Fukushima Daiichi Nuclear Power Plant. *SOLA* 7:101–104.
13. Visible Information Center Inc. (2011) Simulation on ^{137}Cs deposition due to the emission from Fukushima Daiichi Nuclear Plant., Available at: <http://www.vic.jp/fukushima/global/global-e.html>.
14. Japan Atomic Energy Agency (2011) A trial calculation on total amount of radiation exposure during 2 months after the accident of Fukushima Daiichi Nuclear Power Plant in TEPCO., Available at: <http://www.jaea.go.jp/jishin/kaisetsu03/kaisetsu03.htm> (in Japanese).
15. The EURAD project (2011) Potential dispersion of the radioactive cloud over the northern hemisphere., Available at: http://www.eurad.uni-koeln.de/index_e.html.
16. Deutscher Wetterdienst (2011) Deutscher Wetterdienst zu den Folgen der Fukushima-Katastrophe Wetter sorgt für starke Verdünnung der radioaktiven Konzentration., Available at: http://www.dwd.de/bvbw/generator/DWDWWW/Content/Presse/Pressemittelungen/2011/20110323__Japan,templateId=raw,property=publicationFile.pdf/20110323_Japan.pdf.
17. Japanese Ministry of Education, Culture, Sports, Science, and Technology (MEXT) (2011) Reading of radioactivity level in fallout by prefecture., Available at: <http://www.mext.go.jp/english/incident/1305529.htm>.
18. Japanese Ministry of Education, Culture, Sports, Science, and Technology (MEXT) (2011) Readings of sea area monitoring., Available at: <http://www.mext.go.jp/english/incident/1304192.htm>.
19. United Nations Scientific Committee on the Effects of Atomic Radiation (UNSCEAR) (2000) Sources and effects of ionizing radiation. *Sources Annex A*, Vol I (United Nations, New York), Available at: http://www.unscear.org/unscear/en/publications/2000_1.html.
20. Japanese Ministry of Education, Culture, Sports, Science, and Technology (MEXT) (2011) Readings of environmental radioactivity level by prefecture., Available at: <http://www.mext.go.jp/english/incident/1304080.htm>.
21. Japanese Ministry of Education, Culture, Sports, Science, and Technology (MEXT) and the US Department of Energy (DOE) (2011) Results of Airborne Monitoring by the Ministry of Education, Culture, Sports, Science, and Technology and the US Department of Energy., Available at: <http://www.mext.go.jp/english/incident/1304796.htm>.
22. Japanese Ministry of Education, Culture, Sports, Science, and Technology (MEXT) (2011) Environmental radiation database., Available at: <http://search.kankyo-hoshano.go.jp/servlet/search.top>.
23. Tsukada H, Hisamatsu S, Inaba J (2003) Transfer of ^{137}Cs and stable Cs in soil-to-grass-milk pathway in Aomori., Japan. *J Radioanal Nucl Chem* 255:455–458.
24. Ministry of Agriculture, Forestry, and Fisheries (MAFF) (2011) A point of view on planting rice plant., Available at: http://www.maff.go.jp/j/kanbo/joho/saigai/pdf/ine_sakutuke.pdf (in Japanese).
25. Holland DM (2000) Merged IBCAO/ETOPO5 global topographic data product. *National Geophysical Data Center (NGDC), Boulder Colorado*, Available at: http://efdl.cims.nyu.edu/project_aomip/forcing_data/topography/merged/overview.html.
26. Japanese Ministry of Education, Culture, Sports, Science, and Technology (MEXT) (2011) Calculation results and basis regarding internal exposure studied in summarizing the tentative approach., Available at: http://www.mext.go.jp/component/english/_icsFiles/afiedfile/2011/05/27/1306601_0512_1.pdf.

Supporting Information

Yasunari et al. 10.1073/pnas.1112058108

SI Text

Data of Japanese Prefecture Boundaries. The data of Japanese prefecture boundaries for plotting Figs. 1–3, and Figs. S1, S4, and S6 and Movies S1–S4 were obtained from the following web site: http://www.geocities.jp/ne_o_t/GMT-USE/use-medium/ken.txt.

Details of Dispersion Model Setup. Cesium-137 was simulated using FLEXPART (1) as an aerosol with lognormal size distribution (0.6 μm mean diameter and standard deviation of 0.3). Scavenging coefficients were set to $A = 10^{-4} \text{ s}^{-1}$ for precipitation of 1 mm h^{-1} and a dependency on precipitation rate of $B = 0.80$ (see ref. 1 for an explanation of these parameters). The source strength was constant throughout the period of simulation. Preliminary comparisons with global radionuclide monitoring data suggests that FLEXPART's atmospheric ^{137}Cs concentrations drop off too quickly with distance, likely because of an overestimation of wet deposition. Given that FLEXPART deposition fields are not used in terms of absolute numbers here, not impacting our results strongly. However, proximal deposition values may tend to be too high, whereas distal deposition values may tend to be too low.

Deposition Ratio (DR). Although FLEXPART (1) can treat the transport and deposition process of ^{137}Cs , constant emission from the Fukushima Daiichi NPP was assumed similar to some other studies of this event (2–8) because of missing emission source information. Therefore, using direct deposition fields from FLEXPART is not reliable and we computed relative ^{137}Cs deposition distributions by normalizing the FLEXPART output by the maximum values within the output domain. The normalized output is DR and shows the potential areas of relatively high ^{137}Cs deposition. An example of three-hourly DR maps are shown in Movie S1. In the daily DR calculation, although the effect is negligible, we corrected negative deposition values to zero deposition because of the decay process after a little deposition on the ground. The deposition outputs in each time interval are the difference between two subsequent accumulated fields.

Note on the Root Mean Square Errors (RMSEs) of the Estimated ^{137}Cs Depositions. The RMSEs between observed daily ^{137}Cs deposition in each prefecture and the estimated daily deposition were also computed using the observations on available days between March 20 and April 19 (Fig. S2). When using DR threshold (DRT) = 0.005 during the period, the RMSEs of estimated ^{137}Cs deposition were less than 1,232.3 MBq km^{-2} (Fig. S2). Miyagi prefecture had no observation on the deposition during the period and the RMSE could have not estimated. Yamagata and Fukushima prefectures had missing data and these two important observatories probably do not show actual total depositions and underestimated real deposition amounts between March 20 and April 19 (Fig. 2B).

Note on DRT. Our estimates are an observation-based reconstruction of the ^{137}Cs deposition distribution for all of Japan. Although our method is sensitive to the choice of DRT, we tested various DRT values to determine realistic deposition ranges (Fig. S2 and Table S3). The DRT values were determined covering 0.1–10% (0.001, 0.005, 0.007, 0.01, 0.05, and 0.1) of the daily DR maximum (DR = 1). To estimate ^{137}Cs deposition between March 20 and April 19, we concluded that DRT values between 0.005 and 0.01 best explain the observed deposition in main prefectures because the estimates using DRT of 0.001 and 0.05–0.1 showed extremely high RMSEs in some prefectures (Fig. S2). From the viewpoint of precautionary principle, overestimates may be better than underestimates and, thus, we adopted DRT = 0.005 for our best guess estimates of the deposition distribution between March 20 and April 19. In most prefectures of western Japan, ^{137}Cs depositions were not detected at the locations of the observatories during this period. Our estimates using DRT = 0.005 resulted in deposition of less than 50 MBq km^{-2} in many prefectures of western Japan (Table S3), which roughly represents the uncertainty of our method. Therefore, it seems entirely possible that western Japan was not at all effected by noticeable amounts of ^{137}Cs deposition. Comparisons of future observations with our estimates are essential for a more robust assessment.

Note on Soil Contamination. It is worthwhile to note that the case for DRT = 0.001 is closer to the direct soil observations than results for DRT = 0.005 (Fig. 4), our best guess estimate for the total ^{137}Cs deposition between March 20 and April 19 (Fig. 2A). The estimates on the soil contamination from daily deposition observations also showed lower concentrations than those of direct soil observations because the time period in our simulation and observation-based estimate in deposition did not include the period before March 20 and sometimes after April 19, whereas soil samples include the information before March 20 including the period just after the nuclear power plant accident and also after April 19 in some samples as mentioned in the main text. Hence, it is reasonable to say that ^{137}Cs concentration from direct soil samples did show some higher concentrations of ^{137}Cs than our deposition-based estimates for the period between March 20 and April 19. In Fukushima City where deposition observation was carried out, the estimated ^{137}Cs concentration in soil using DRT of 0.001 was closest to the observations but still was somewhat underestimated (Fig. 4A). Although our estimate is limited to the period between March 20 and April 19, the estimated soil contamination on ^{137}Cs using DRT of 0.001 are relatively well reconstructed compared to the sporadic soil observations beyond the time period, probably considering the contributions to the total ^{137}Cs depositions before March 20 (Fig. 4). This discussion is similar to the one for the deposition in the main text.

1. Stohl A, Forster C, Frank A, Seibert P, Wotawa G (2005) The Lagrangian particle dispersion model FLEXPART, version 6.2. *Atmos Chem Phys* 5:2461–2474.
2. Japanese Ministry of Education, Culture, Sports, Science and Technology (MEXT) (2011) System for prediction of environment emergency dose information (SPEEDI). Available at: http://www.nsc.go.jp/mext_speedi/index.html (in Japanese).
3. Japan Meteorological Agency (2011) Environmental emergency response. Available at: http://www.jma.go.jp/jma/kokusaieer_list.html.
4. Takemura T. et al. (2011) A numerical simulation of global transport of atmospheric particles emitted from the Fukushima Daiichi Nuclear Power Plant. *SOLA* 7:101–104.
5. Visible Information Center Inc. (2011) Simulation on ^{137}Cs deposition due to the emission from Fukushima Daiichi Nuclear Plant. Available at: <http://www.vic.jp/fukushima/global/global-e.html>.
6. Japan Atomic Energy Agency (2011) A trial calculation on total amount of radiation exposure during 2 month after the accident of Fukushima Daiichi Nuclear Power Plant in TEPCO. Available at: <http://www.jaea.go.jp/jishin/kaisetsu03/kaisetsu03.html> (in Japanese).
7. The EURAD project (2011) Potential dispersion of the radioactive cloud over the northern hemisphere. Available at: http://www.eurad.uni-koeln.de/index_e.html.
8. Deutscher Wetterdienst (2011) Deutscher Wetterdienst zu den Folgen der Fukushima-Katastrophe Wetter sorgt für starke Verdünnung der radioaktiven Konzentration. Available at: http://www.dwd.de/bvbw/generator/DWDWWW/Content/Presse/Pressemittelungen/2011/20110323_Japan,templateId=raw,property=publicationFile.pdf/20110323_Japan.pdf.

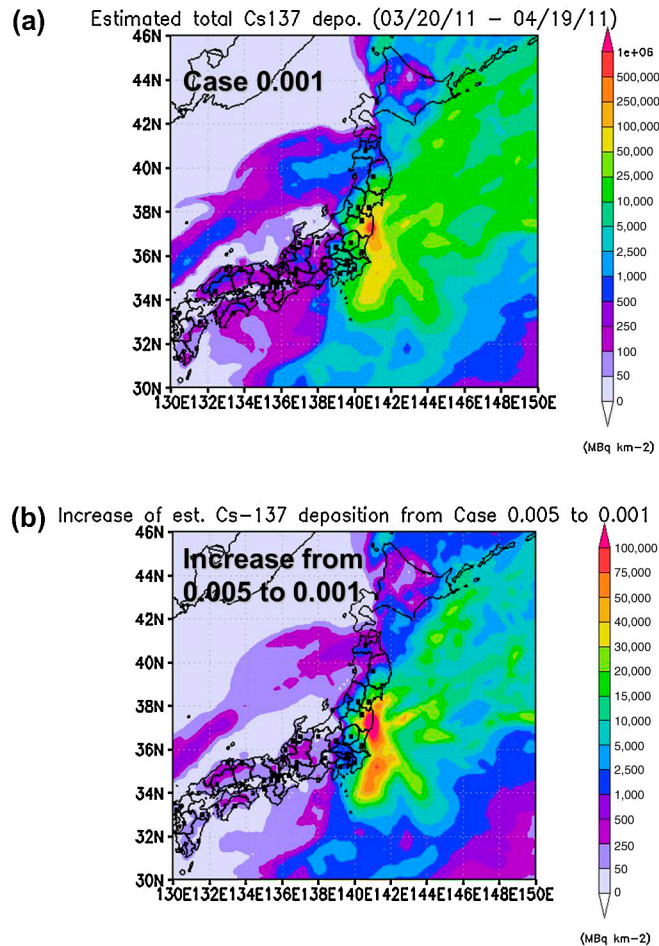


Fig. S4. Comparison between estimates of total ^{137}Cs deposition using different DRT. (A) Estimated total ^{137}Cs deposition using DRT of 0.001. (B) Increase of estimated total ^{137}Cs deposition from using DRT of 0.005 to 0.001. Squares in black denote the locations of the observatories in each prefecture (Table S2). Outputs with $0.2^\circ \times 0.2^\circ$ in the daily estimates were interpolated into finer resolution using cubic interpolation.

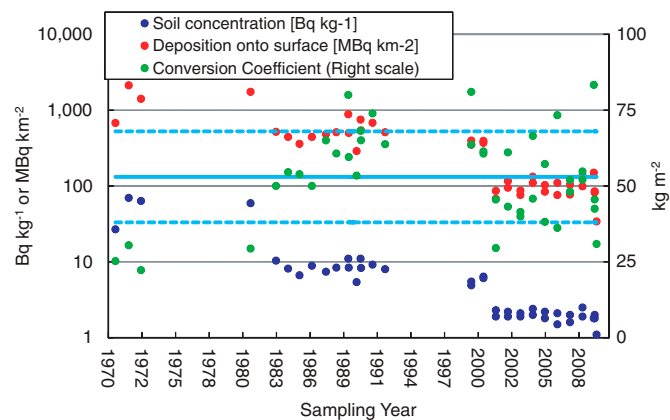
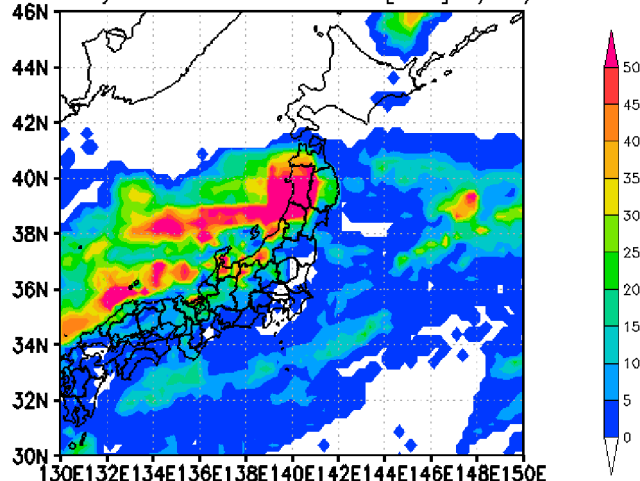


Fig. S5. Relationship between ^{137}Cs deposition and concentration in soil for determining conversion coefficient (CC). The historical observed data were obtained from the environmental radiation database (1) maintained by the Japan Chemical Analysis Center. The observed data at the same location and on the same day in different units of Bq kg^{-1} (top 5 cm soil) and MBq km^{-2} (Bq m^{-2}) are assumed to be the same sample and used the data for calculating the CC (kg m^{-2}). Solid and dotted lines denote mean CC value and its standard deviations, respectively.

1 Japanese Ministry of Education, Culture, Sports, Science, and Technology (MEXT) (2011). Environmental radiation database. Available at: <http://search.kankyo-hoshano.go.jp/servlet/search.top>.

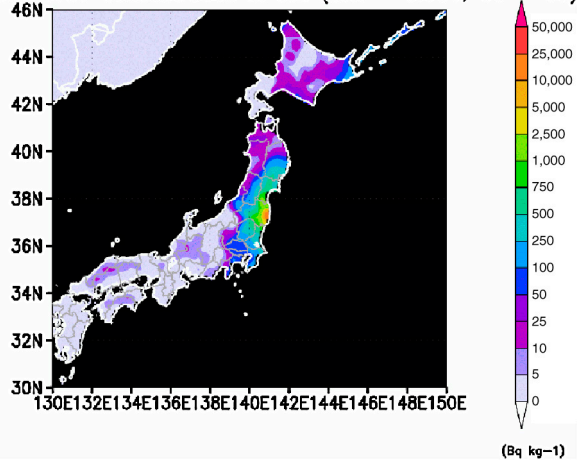
TRMM Daily Accumulated Rainfall [mm] 3/20/2011



Movie S3. Daily accumulated precipitation by tropical rainfall measuring mission (TRMM, 3B42 V6 product) satellite data.

[Movie S3 \(MOV\)](#)

Estimated Cs137 concentration in soil (DRT = 0.001; CC = 68)



Movie S4. Estimated ^{137}Cs concentration range in soil using DRT of 0.001 and conversion coefficient (CC) of 38, 53, and 68 kg m^{-2} over Japan. CCs of 38, 53, and 68 kg m^{-2} correspond to -1σ , mean value, and $+1\sigma$ in Fig. S5, respectively. Outputs $0.2^\circ \times 0.2^\circ$ were interpolated into finer resolution using cubic interpolation. The Merged IBCAO/ETOPO5 Global Topographic Data Product (1) was used to mask out ocean area below 0 m above sea level (a.s.l.).

1 Holland, DM (2000) Merged IBCAO/ETOPO5 Global Topographic Data Product. National Geophysical Data Center (NGDC), Boulder Colorado. Available at: http://efdl.cims.nyu.edu/project_aomip/forcing_data/topography/merged/overview.html.

[Movie S4 \(MOV\)](#)

Table S1. Data sources for observed ¹³⁷Cs concentrations in soil or grass in selected prefectures

	Sample	Sample type	Source
Hokkaido	April 18, 19, 25	Soil	http://www.pref.hokkaido.lg.jp/ns/gjff/dojomonitoring230428.pdf
Aomori	May 18	Grass	http://www.pref.aomori.lg.jp/soshiki/nourin/chikusan/files/grass-radi.pdf
Iwate	May 11	Grass	http://www.pref.iwate.jp/download.rbz?cmd=50&cd=32320&tg=3
Miyagi	May 11, 18, 19	Grass	http://www.pref.miyagi.jp/tikusanka/0400-souchishiryu/110525pr2.pdf
Akita	May 14	Grass	http://www.pref.akita.lg.jp/www/contents/1305379159624/files/kekka.pdf
Yamagata	April 2, 18, 22	Soil	http://www.pref.yamagata.jp/ou/norinsuisan/140027/hosya-press_release/0506dojokekka.pdf http://www.pref.yamagata.jp/ou/seikatsukankyo/050014/radiation/dojou.pdf
Fukushima*	April 14	School soil	http://radioactivity.mext.go.jp/en/1380/2011/04/1305394_0419_1.pdf
	April 20 [†]	Soil	http://radioactivity.mext.go.jp/en/monitoring_around_FukushimaNPP_soil_monitoring/2011/05/1306622_053110.pdf
Ibaraki	April 8	Soil	http://www.pref.ibaraki.jp/important/20110311eq/20110408_20/files/20110408_20a.pdf
Tochigi	April 8	Soil	http://www.pref.tochigi.lg.jp/kinkyu/houshanou_suiden.html
Gunma	April 1, 2	Soil	http://www.pref.gunma.jp/houdou/f1000020.html
Saitama [‡]	April 22	Grass	http://www.maff.go.jp/j/kanbo/joho/saigai/syohu/bokusou_kensa.html#saitama
Chiba	April 21 [§]	Grass	http://www.maff.go.jp/j/kanbo/joho/saigai/syohu/bokusou_kensa.html#tiba
	March 31	Soil	http://www.pref.chiba.lg.jp/annou/h23touhoku/suidendojo.html
Tokyo [¶]	April 10, 16	Soil	http://prayforjp.exblog.jp/13594347 http://savechild.net/wp-content/uploads/2011/05/300467512.jpg
Kanagawa	March 25, 30 and May 16, 17	Soil	http://www.pref.kanagawa.jp/cnt/f300508/
Niigata	April 11	Soil	http://www.bousai.pref.niigata.jp/contents/dbps_data/_material/_localhost/704.pdf

* Observed by prefecture, unless where indicated.

[†] Observed by Ministry of Education, Culture, Sports, Science, and Technology (MEXT).

[‡] Samples picked up before April 20. In the samples, we excluded the data with *3 of top 5-mm soil sample.

[§] Observed by Ministry of Agriculture, Forestry, and Fisheries (MAFF). Only April 22 samples were used.

[¶] Observed by MAFF. Only April 21 samples were used.

[¶] Observed by Prof. Yamazaki et al. at Kinki University and published in the Asahi newspaper on May 15. These sources are an example of data available in the Asahi newspaper.

Table S2. Observatory locations in each prefecture

Prefecture	Grid box X	Grid box Y
Hokkaido	107	91
Aomori	104	80
Iwate	106	74
Miyagi	105	67
Akita	101	74
Yamagata	102	67
Fukushima	103	64
Ibaraki	103	57
Tochigi	100	59
Gunma	96	58
Saitama	99	55
Chiba	101	53
Tokyo	99	54
Kanagawa	97	52
Niigata	95	65
Toyama	86	59
Ishikawa	84	58
Fukui	82	56
Yamanashi	93	54
Nagano	91	59
Gifu	85	53
Shizuoka	91	49
Aichi	85	52
Mie	83	50
Shiga	80	50
Kyoto	79	50
Osaka	78	49
Hyogo	76	49
Nara	80	49
Wakayama	76	47
Tottori	70	53
Shimane	66	53
Okayama	70	48
Hiroshima	63	48
Yamaguchi	58	46
Tokushima	73	46
Kagawa	71	47
Ehime	63	43
Kochi	68	43

Prefecture	Grid box X	Grid box Y
Fukuoka	53	43
Saga	52	42
Nagasaki	50	40
Kumamoto	54	39
Oita	59	41
Miyazaki	58	35
Kagoshima	53	33
Okinawa	39	6

Grid numbers of X and Y correspond to the grid boxes of the observatories (X, Y) within 0.2° × 0.2° horizontal resolution domain starting from 120°E to eastward and from 25°N to northward. Although Miyagi did not observe any deposition during the time period in this paper, the location for atmospheric radiation measurement in Miyagi was temporarily put here for our calculation process.

Table S3. Comparisons of ¹³⁷Cs depositions at each observatory location in each prefecture between March 20 and April 19

(MBq km ⁻²)	Hokkaido	Aomori	Iwate	Miyagi	Akita	Yamagata	Fukushima	Ibaraki
Sum of observations	2.3	0.0	795.8	N/A	24.5	8,622.9	2,196.7	28,429.7
Case 0.1 estimate	13.0	23.8	2,301.3	7,607.6	137.5	3,398.1	4,085.9	6,482.1
Case 0.05 estimate	13.1	47.5	2,101.6	9,417.3	167.7	3,853.0	5,572.0	7,158.5
Case 0.01 estimate	14.0	213.6	3,285.7	21,704.7	309.1	6,854.2	14,055.0	14,923.2
Case 0.007 estimate	14.3	297.7	3,533.8	25,253.8	354.1	7,566.3	17,209.5	16,786.8
Case 0.005 estimate	16.0	401.7	3,800.6	28,458.6	366.6	8,356.1	19,619.0	18,036.1
Case 0.001 estimate	74.4	1,252.4	5,939.0	54,284.8	415.9	15,008.7	43,428.3	27,248.9
(MBq km ⁻²)	Tochigi	Gunma	Saitama	Chiba	Tokyo	Kanagawa	Niigata	Toyama
Sum of observations	2,669.1	1,302.8	3,752.7	4,844.1	6,872.5	550.2	15.0	0.0
Case 0.1 estimate	4,583.0	1,801.9	2,244.5	1,584.6	1,328.5	343.4	8.4	1.3
Case 0.05 estimate	5,311.3	1,963.3	2,529.2	1,754.3	1,653.2	565.4	14.3	2.5
Case 0.01 estimate	9,274.4	2,172.9	3,488.6	2,103.1	2,640.9	1,502.5	48.6	9.0
Case 0.007 estimate	10,423.8	2,043.5	3,968.8	2,219.3	3,026.5	1,830.2	63.5	11.6
Case 0.005 estimate	11,519.0	1,949.8	4,200.0	2,460.1	3,221.8	2,091.0	77.2	13.4
Case 0.001 estimate	21,525.7	2,358.7	6,256.5	4,847.8	4,936.9	5,189.2	232.6	25.3
(MBq km ⁻²)	Ishikawa	Fukui	Yamanashi	Nagano	Gifu	Shizuoka	Aichi	Mie
Sum of observations	0.0	3.9	114.6	0.0	4.7	127.3	0.0	0.0
Case 0.1 estimate	4.1	7.8	46.5	3.9	7.4	45.6	4.9	7.6
Case 0.05 estimate	7.9	14.2	61.7	7.5	12.9	73.5	9.3	13.6
Case 0.01 estimate	30.1	54.0	127.3	26.0	45.9	204.0	32.9	42.4
Case 0.007 estimate	39.2	70.1	137.3	33.0	59.5	247.5	41.4	48.4
Case 0.005 estimate	48.1	88.3	141.1	36.7	73.8	273.6	48.1	51.0
Case 0.001 estimate	117.7	251.1	158.2	55.6	185.1	446.9	96.7	64.6
(MBq km ⁻²)	Shiga	Kyoto	Osaka	Hyogo	Nara	Wakayama	Tottori	Shimane
Sum of observations	0.0	0.0	0.0	0.0	0.0	0.0	0.0	0.0
Case 0.1 estimate	3.6	4.1	2.1	3.5	3.1	4.0	8.6	1.8
Case 0.05 estimate	6.7	7.8	4.1	6.8	5.7	7.6	16.6	3.6
Case 0.01 estimate	24.5	30.0	15.3	25.9	20.2	26.0	61.0	18.0
Case 0.007 estimate	31.1	39.1	19.9	33.9	25.0	32.6	79.3	25.6
Case 0.005 estimate	37.1	48.4	24.0	41.6	29.2	36.1	93.1	35.7
Case 0.001 estimate	91.0	135.7	65.7	107.6	70.8	63.0	224.0	154.0
(MBq km ⁻²)	Okayama	Hiroshima	Yamaguchi	Tokushima	Kagawa	Ehime	Kochi	Fukuoka
Sum of observations	0.0	0.0	0.0	0.0	0.0	0.0	2.4	0.0
Case 0.1 estimate	1.6	4.4	0.6	5.7	1.8	2.4	24.5	0.4
Case 0.05 estimate	3.1	8.8	1.2	10.2	3.3	4.6	41.3	0.8
Case 0.01 estimate	11.4	43.6	5.9	35.6	12.3	20.8	123.0	4.2
Case 0.007 estimate	14.6	62.2	8.5	43.1	15.4	28.8	130.5	6.0
Case 0.005 estimate	17.5	87.0	11.8	51.0	18.9	38.4	137.0	8.5
Case 0.001 estimate	44.6	390.8	51.4	141.5	58.0	154.7	201.0	38.3
(MBq km ⁻²)	Saga	Nagasaki	Kumamoto	Oita	Miyazaki	Kagoshima	Okinawa	
Sum of observations	0.0	0.0	0.0	0.0	0.0	0.0	0.0	
Case 0.1 estimate	0.4	0.4	0.3	1.4	0.6	0.5	0.0	
Case 0.05 estimate	0.8	0.7	0.5	2.8	1.2	1.0	0.1	
Case 0.01 estimate	4.0	3.4	2.5	13.8	5.9	4.8	0.4	
Case 0.007 estimate	5.6	4.9	3.6	19.8	8.4	6.8	0.6	
Case 0.005 estimate	7.9	6.8	5.1	27.7	11.7	9.5	0.8	
Case 0.001 estimate	35.6	30.4	22.7	126.1	53.3	43.3	3.6	

Table S4. Comparisons of ¹³⁷Cs contamination in soil at each observatory location in each prefecture [conversion coefficient (CC) = 53 kg m⁻²]

(Bq kg ⁻¹)	Hokkaido	Aomori	Iwate	Miyagi	Akita	Yamagata	Fukushima	Ibaraki
Sum of observations	0.0	0.0	15.0	N/A	0.5	162.7	41.4	536.4
Case 0.1 estimate	0.2	0.4	43.4	143.5	2.6	64.1	77.1	122.3
Case 0.05 estimate	0.2	0.9	39.7	177.7	3.2	72.7	105.1	135.1
Case 0.01 estimate	0.3	4.0	62.0	409.5	5.8	129.3	265.2	281.6
Case 0.007 estimate	0.3	5.6	66.7	476.5	6.7	142.8	324.7	316.7
Case 0.005 estimate	0.3	7.6	71.7	537.0	6.9	157.7	370.2	340.3
Case 0.001 estimate	1.4	23.6	112.1	1,024.2	7.8	283.2	819.4	514.1
(Bq kg ⁻¹)	Tochigi	Gunma	Saitama	Chiba	Tokyo	Kanagawa	Niigata	Toyama
Sum of observations	50.4	24.6	70.8	91.4	129.7	10.4	0.3	0.0
Case 0.1 estimate	86.5	34.0	42.3	29.9	25.1	6.5	0.2	0.0
Case 0.05 estimate	100.2	37.0	47.7	33.1	31.2	10.7	0.3	0.0
Case 0.01 estimate	175.0	41.0	65.8	39.7	49.8	28.3	0.9	0.2
Case 0.007 estimate	196.7	38.6	74.9	41.9	57.1	34.5	1.2	0.2
Case 0.005 estimate	217.3	36.8	79.2	46.4	60.8	39.5	1.5	0.3
Case 0.001 estimate	406.1	44.5	118.0	91.5	93.1	97.9	4.4	0.5
(Bq kg ⁻¹)	Ishikawa	Fukui	Yamanashi	Nagano	Gifu	Shizuoka	Aichi	Mie
Sum of observations	0.0	0.1	2.2	0.0	0.1	2.4	0.0	0.0
Case 0.1 estimate	0.1	0.1	0.9	0.1	0.1	0.9	0.1	0.1
Case 0.05 estimate	0.1	0.3	1.2	0.1	0.2	1.4	0.2	0.3
Case 0.01 estimate	0.6	1.0	2.4	0.5	0.9	3.8	0.6	0.8
Case 0.007 estimate	0.7	1.3	2.6	0.6	1.1	4.7	0.8	0.9
Case 0.005 estimate	0.9	1.7	2.7	0.7	1.4	5.2	0.9	1.0
Case 0.001 estimate	2.2	4.7	3.0	1.0	3.5	8.4	1.8	1.2
(Bq kg ⁻¹)	Shiga	Kyoto	Osaka	Hyogo	Nara	Wakayama	Tottori	Shimane
Sum of observations	0.0	0.0	0.0	0.0	0.0	0.0	0.0	0.0
Case 0.1 estimate	0.1	0.1	0.0	0.1	0.1	0.1	0.2	0.0
Case 0.05 estimate	0.1	0.1	0.1	0.1	0.1	0.1	0.3	0.1
Case 0.01 estimate	0.5	0.6	0.3	0.5	0.4	0.5	1.2	0.3
Case 0.007 estimate	0.6	0.7	0.4	0.6	0.5	0.6	1.5	0.5
Case 0.005 estimate	0.7	0.9	0.5	0.8	0.6	0.7	1.8	0.7
Case 0.001 estimate	1.7	2.6	1.2	2.0	1.3	1.2	4.2	2.9
(Bq kg ⁻¹)	Okayama	Hiroshima	Yamaguchi	Tokushima	Kagawa	Ehime	Kochi	Fukuoka
Sum of observations	0.0	0.0	0.0	0.0	0.0	0.0	0.0	0.0
Case 0.1 estimate	0.0	0.1	0.0	0.1	0.0	0.0	0.5	0.0
Case 0.05 estimate	0.1	0.2	0.0	0.2	0.1	0.1	0.8	0.0
Case 0.01 estimate	0.2	0.8	0.1	0.7	0.2	0.4	2.3	0.1
Case 0.007 estimate	0.3	1.2	0.2	0.8	0.3	0.5	2.5	0.1
Case 0.005 estimate	0.3	1.6	0.2	1.0	0.4	0.7	2.6	0.2
Case 0.001 estimate	0.8	7.4	1.0	2.7	1.1	2.9	3.8	0.7
(Bq kg ⁻¹)	Saga	Nagasaki	Kumamoto	Oita	Miyazaki	Kagoshima	Okinawa	
Sum of observations	0.0	0.0	0.0	0.0	0.0	0.0	0.0	
Case 0.1 estimate	0.0	0.0	0.0	0.0	0.0	0.0	0.0	
Case 0.05 estimate	0.0	0.0	0.0	0.1	0.0	0.0	0.0	
Case 0.01 estimate	0.1	0.1	0.0	0.3	0.1	0.1	0.0	
Case 0.007 estimate	0.1	0.1	0.1	0.4	0.2	0.1	0.0	
Case 0.005 estimate	0.1	0.1	0.1	0.5	0.2	0.2	0.0	
Case 0.001 estimate	0.7	0.6	0.4	2.4	1.0	0.8	0.1	